Applied Mathematics and Computation 439 (2023) 127628

Contents lists available at ScienceDirect

Applied Mathematics and Computation

journal homepage: www.elsevier.com/locate/amc

Some qualitative properties of the discrete models for malaria propagation

I. Faragó [a,b,c], R. Mosleh [a,*]

[a] Department of Differential Equations at Budapest University of Technology and Economics, Hungary
[b] Department of Applied Analysis and Computational Mathematics at Eötvös Loránd University, Hungary
[c] Numerical Analysis and Large Networks Research Group at ELKH-ELTE, Hungary

ARTICLE INFO

Article history:
Received 24 May 2021
Revised 10 August 2022
Accepted 7 October 2022

Keywords:
Ross-Macdonald model
Extended Ross model
Positively invariant
Positivity preservation
Malaria propagation
Step-size function
Dynamical consistency
Nonlcal discretization

ABSTRACT

This paper addresses a reliable mathematical modeling of malaria propagation in infected societies for humans and mosquitoes with an extension of the basic Ross–Macdonald model. We analyze the extended Ross model numerically which is an initial value problem of a seven-dimensional system of the first-order ODEs. For this aim, the discretized scheme of the extended model is split into two parts. First, we apply the step-size functions to approximate the time derivatives with the first-order consistency. Then we use a nonlocal discretization of the standard θ-method to the right side of the system to obtain a linear system. We find the conditions for the step-size functions under which specific intervals are positively invariant for the total populations and each component of the solution of the extended Ross model. We suggest a step-size function for the extended Ross model to preserve the dynamical consistency of the model for any step size Δt. The numerical simulations confirm the theoretical results for the examples and we compare the efficiency of the nonstandard Runge–Kutta methods with the different step-size functions for sufficiently large step sizes.

1. Introduction

Nowadays that most people are struggling with COVID-19 pandemic throughout the world, there are other types of epidemics that human beings have been dealing with them for ages such as malaria which is an infectious and deadly disease spread to humans as hosts by female Anopheles mosquitoes as vectors. This phenomenon, which is endemic in tropical and subtropical regions appertains greatly to the climate factors such as temperature, altitude, precipitation, and raised humidity. Moreover, global warming and climate change increase this incident. Other various reasons are responsible for the latest malaria upsurge, such as drug resistance, mosquito control programs, public health facilities, and living standards. Nevertheless, since there is no effective vaccine, it is crucial to analyze its mechanism [1,18,22].

Reliable mathematical modeling of epidemics transmission is a key tool for getting a better insight into the disease, prevent them from contagion in the future, and reduce their impacts in the real life. For this aim, a variety of mathematical models have been brought up to interpret malaria transmission. Ronald Ross was a pioneer in this field [21] and his model

* Corresponding author.
E-mail address: rmosleh028@gmail.com (R. Mosleh).

https://doi.org/10.1016/j.amc.2022.127628

was further studied by George Macdonald, however, their model fails to sketch an adequate model [7,17]. Therefore, we consider an extension of the basic Ross–Macdonald model to take into account more effective factors in malaria transmission.

A lot of literature discusses various mathematical modelings for malaria transmission [8,10,24]. This paper analyzes a dynamical system, the extended Ross model, for malarial propagation in numerical details.

The extended Ross model is an SEIRS–type model interpreted by a seven-dimensional system of nonlinear ODEs. Analytically, it is proved that the continuous extended Ross model is well-posed and it has several qualitative properties. It is worth to mention that these properties are motivated by the original modeled process, which is in our case the epidemic propagation. Such a property is e.g. that some specific intervals are positively invariant for the total populations and each component of the solution [5]. Since finding an analytic solution for this model is rigid, we mainly consider numerical methods. This paper focuses on dynamical consistency, which means that main characteristic properties of continuous models are preserved on numerical levels. Hence, we extend the standard finite difference discretization technique by applying some suitably chosen step-size functions to approximate the time derivatives. For this goal, we discuss some specific properties for the step-size functions to approximate the time derivatives with the first-order consistency. As the system is highly nonlinear, we apply a nonlocal discretization of the standard θ-method to the right side of the system to obtain a linear system. Since the extended Ross model is a dynamical system and behavior of the system on sufficiently large time intervals is important, small step sizes Δt are not applicable. Hence, we suggest a step-size function for the extended Ross model which guarantees the dynamical consistency for the extended Ross model for any step size Δt. The suggested step-size function improves the accuracy and absolute stability of the explicit Runge–Kutta methods and preserves the order of the standard Runge–Kutta methods [13]. This method is substantially similar to the nonstandard positive schemes called as BBKS, MPRK and GeCo (see e.g. [2,11,13]) to profit the dynamical consistency unconditionally. These methods, usually applied to the biochemical systems, preserve the positivity of the solutions unconditionally for the step sizes and do not discuss the upper bounds of the solutions, while the present method considers the uniformly bounded solutions. Moreover, these methods make a profit from the mass-conservative property of the system in the strict case (when the model focuses on the constant mass over the reactions and there is no input and output mass to the system).

The present paper is organised as follows, in the next section, we compare the structure and properties of the basic Ross–Macdonald model with the extended Ross model. Section 3 mainly, focuses on the discrete scheme of the extended Ross model. In Section 3.1, we extend the standard finite difference discretization and we apply the step-size functions to approximate the time derivatives with the first-order consistency. Section 3.2 applies a nonlocal discretization of the standard θ-method to the right side of the system to obtain a linear system. Sections 3.3 and 3.4 seek the conditions under which the dynamical consistency is valid. In Section 3.5, we find suitable domains for the step-size functions in such a way the dynamical consistency is valid. In Section 4, we give some numerical examples to verify the theoretical results and investigate the sharpness of the bounds.

2. Continuous models of ODEs for malaria propagation

The Ross–Macdonald model, the most preliminary model to interpret malaria transmission [21], is a dynamical system formulated as

$$\begin{cases} \dot{S}_h(t) = dN_h + rI_h(t) - b\beta_h S_h(t)\frac{I_m(t)}{N_h} - dS_h(t) \\ \dot{I}_h(t) = b\beta_h S_h(t)\frac{I_m(t)}{N_h} - (r+d)I_h(t) \\ \dot{S}_m(t) = \mu N_m - b\beta_m S_m(t)\frac{I_h(t)}{N_h} - \mu S_m(t) \\ \dot{I}_m(t) = b\beta_m S_m(t)\frac{I_h(t)}{N_h} - \mu I_m(t), \end{cases} \tag{1}$$

with the initial data

$$\begin{cases} S_h(0) = S_{0h},\ I_h(0) = I_{0h}, \\ S_m(0) = S_{0m},\ I_m(0) = I_{0m}. \end{cases} \tag{2}$$

Here $S_h(t)$ and $S_m(t)$ signify the number of susceptible humans and mosquitoes at time t, respectively. $I_h(t)$ and $I_m(t)$ are the number of infected humans and mosquitoes at time t, respectively. The parameter b is the rate of mosquito biting, β_h is the probability that a bite from an infected mosquito will cause infection of a susceptible human, and β_m is the probability that a bite from a susceptible mosquito to an infected human individual will cause infection of the mosquito. The parameter r is the recovery rate for humans, d and μ are the birth and mortality rates for humans and mosquitoes, respectively.

The numbers of the total populations for humans and mosquitoes, N_h and N_m, are constant defining as

$$S_h(t) + I_h(t) = N_h, \tag{3}$$

and

$$S_m(t) + I_m(t) = N_m, \tag{4}$$

respectively. According to (3) and (4), we can reduce and re-scale the system (1) and (2) for which the solution is density. Hence, it should take values on the interval [0,1]. This property is considered analytically and numerically in [6]. In this model, the number of the populations are assumed to be constant, the exposed states for humans and mosquitoes, and

the recovery state for humans are not considered. Moreover, the force of infections for humans and mosquitoes, $\frac{b\beta_h I_m(t)}{N_h}$ and $\frac{b\beta_m I_h(t)}{N_h}$, are linear concerning $I_m(t)$ and $I_h(t)$, respectively and do not consider the saturating feature of the infection. Due to these drawbacks, the basic Ross–Macdonald model fails to interpret an adequate model for malaria transmission. For the rectification, we study an extension of the basic Ross–Macdonald model and expound on a more appropriate model for malarial propagation. The extended Ross model splits the human population into four subclasses containing susceptible humans, exposed humans, infectious humans, and recovered humans whereas, the mosquito population is divided into the first three subclasses since the mosquitoes demise after the infection. From the biological standpoint, the extended Ross model is framed as below [19]:

$$\begin{cases} \dot{S}_h(t) = \Lambda_h - \frac{b\beta_h S_h(t) I_m(t)}{1+\nu_h I_m(t)} - \mu_h S_h(t) + \omega R_h(t) \\ \dot{E}_h(t) = \frac{b\beta_h S_h(t) I_m(t)}{1+\nu_h I_m(t)} - (\alpha_h + \mu_h) E_h(t) \\ \dot{I}_h(t) = \alpha_h E_h(t) - (r + \mu_h + \delta_h) I_h(t) \\ \dot{R}_h(t) = r I_h(t) - (\mu_h + \omega) R_h(t) \\ \dot{S}_m(t) = \Lambda_m - \frac{b\beta_m S_m(t) I_h(t)}{1+\nu_m I_h(t)} - \mu_m S_m(t) \\ \dot{E}_m(t) = \frac{b\beta_m S_m(t) I_h(t)}{1+\nu_m I_h(t)} - (\alpha_m + \mu_m) E_m(t) \\ \dot{I}_m(t) = \alpha_m E_m(t) - (\mu_m + \delta_m) I_m(t), \end{cases} \tag{5}$$

the initial conditions are denoted as below:

$$\begin{cases} S_h(0) = S_{0h},\ I_h(0) = I_{0h},\ E_h(0) = E_{0h},\ R_h(0) = R_{0h}, \\ S_m(0) = S_{0m},\ E_m(0) = E_{0m},\ I_m(0) = I_{0m}. \end{cases} \tag{6}$$

Here the functions $E_h(t)$ and $E_m(t)$ describe the number of the exposed humans and mosquitoes at time t, respectively. The function $R_h(t)$ is the number of the recovered humans at time t.

Model (5) possesses the population dynamics with the various birth and mortality rates. We assume that all the newly born children are healthy and susceptible and the birth rates $(\Lambda_h,\ \Lambda_m)$ are inputs appended to the susceptible classes.

When the latency periods end for the susceptible individuals who already transferred to the exposed states, the exposed humans and mosquitoes move to the infected classes with the rates $(\alpha_h,\ \alpha_m)$, respectively. The natural mortality rates, $(\mu_h,\ \mu_m)$, are defined for each class of humans and mosquitoes. Besides the natural mortality rates, the infected humans and mosquitoes classes are decreased by the disease death rates, $(\delta_h,\ \delta_m)$, respectively. The infected humans transmit to the recovered class and after a while, the individuals lose the immunity and become vulnerable again by the ω pace. The ratio $\frac{b\beta_h I_m(t)}{1+\nu_h I_m(t)}$ is the force of infection from infected mosquitoes to susceptible humans in which $\nu_h \in [0, 1]$ refers to the proportion of antibodies generated by infected mosquitoes in human bodies in reaction to the encounter of antigens. This force of infection considers the saturating phenomenon and the role of the immune system against the infection. Similarly, for mosquitoes, $\nu_m \in [0, 1]$ is the proportion of antibodies made by infected humans to the antigens contacted. For demographic reasons, the total population size for humans at time t, $V_h(t)$, is defined as

$$V_h(t) = S_h(t) + E_h(t) + I_h(t) + R_h(t). \tag{7}$$

Similarly, the total population size for mosquitoes at time t is defined as

$$V_m(t) = S_m(t) + E_m(t) + I_m(t). \tag{8}$$

Analytically, it is known that the intervals $\left(0,\ \frac{\Lambda_h}{\mu_h}\right]$ and $\left(0,\ \frac{\Lambda_m}{\mu_m}\right]$are positively invariant sets for the total populations and each component of the solution of the extended Ross model (5) for humans and mosquitoes, respectively [5].

This concept means the following. By the notation $S = \left(0,\ \frac{\Lambda_h}{\mu_h}\right]$ no solution starting inside S can leave S in the future [23].

It is noticeable that if the natural mortality rates vanish, the corresponding intervals are unbounded. As regards finding the analytical solution for the Cauchy problem (5) and (6) is rigid, we apply a numerical method. Suitable numerical methods should preserve the qualitative properties of the models beside the convergence. This property so-called dynamical consistency is the objective of this study. Small step sizes are not beneficial because it is vital to analyze dynamical systems over suitably long time periods. For this aim, we seek the dynamical consistency for the extended Ross model (5) for sufficiently large step sizes.

3. Discrete structure of the extended Ross model

In this section, we analyze the discretized scheme of the extended Ross model (5) and (6). To obtain the discrete model, we discretize the equations in (5). This will be done in two steps. Firstly, we define the time derivative approximation and in the next step, we discretize the right side of (5). We aim to give such a numerical scheme that preserves the positively invariant property for some specific intervals for each component of the solution and total populations for any step size Δt.

3.1. Properties of time derivative approximations for discrete models

Discretization of the continuous models on the mesh

$$W_{\Delta t} = \{t_i = i\Delta t, i = 0, 1, 2, \ldots\}, \tag{9}$$

requires the approximation of the time derivative of the unknown functions of the solution at the mesh-points. This can be done by using the formula

$$\dot{u}(t_i) \approx \frac{y^{i+1} - y^i}{\Phi(\Delta t)}, \tag{10}$$

where y^i denotes the approximation to $u(t_i)$, and $\Phi(\Delta t)$ is some suitably chosen step-size function. In the following, we consider properties of the sufficiently smooth step-size function $\Phi(\Delta t)$ in such a way to approximate $\dot{u}(t)$ properly. Clearly, for the local approximation error we have

$$L(\Delta t) = \frac{u(t_{i+1}) - u(t_i)}{\Phi(\Delta t)} - \dot{u}(t_i), \tag{11}$$

and hence the first order consistency condition

$$L(\Delta t) = O(\Delta t) \tag{12}$$

is satisfied when

$$\Phi(0) = 0, \tag{13}$$

and

$$\dot{\Phi}(0) = 1. \tag{14}$$

Conditions (13) and (14) guarantee the first-order approximation, i.e., $L(\Delta t) = O(\Delta t)$.

Therefore, conditions for the step-size function $\Phi(\Delta t)$ are the following:

1. It is defined for non-negative numbers,
2. It is a sufficiently smooth function,
3. It is positive for all positive arguments,
4. Condition (13) holds, i.e., at the point $\Delta t = 0$ it is zero,
5. Condition (14) holds, i.e. $\dot{\Phi}(0) = 1$.

In the following, we give some examples for the the step-size functions with the above properties.

- The step-size function

$$\Phi(\Delta t) = \Delta t, \tag{15}$$

  constructing the standard finite difference method, satisfies conditions (13) and (14).
- The function

$$\Phi_C(\Delta t) = \frac{1 - e^{-C\Delta t}}{C}, \tag{16}$$

  generating Mickens's nonstandard finite difference method [12,14–16], is satisfied conditions (13) and (14). Here, C is an arbitrary chosen, nonzero constant real number. Some other examples are also known [9].

3.2. Full discretization of the extended Ross model

In the previous subsection, we have defined some approximation in time for the left side of the extended Ross model (5). In this part, we consider the space discretization, i.e. the right side of the model. By applying the standard θ-method to the extended Ross model (5), we obtain a nonlinear system for which we need sub-methods such as Newton or fixed-point iteration methods. These methods suffer some drawbacks and alter the dynamical consistency for some step sizes. To get rid of these gaps, we benefit from the following nonlocal scheme of the standard θ-method, i.e., in the implicit scheme of the standard θ-method, we substitute the prior numerical values rather than the new numerical values for some variables. This modification results in a linear system for which the solution of the system is obtained explicitly without using any sub-methods (Cf. [14,15]). Also, by using the step-size function (10), we obtain the following nonstandard θ-scheme for the

extended Ross model (5) and (6).

$$\begin{cases} \frac{S_h^{i+1}-S_h^i}{\Phi(\Delta t)} = (1-\theta)(\Lambda_h - \frac{b\beta_h S_h^i I_m^i}{1+\nu_h I_m^i} - \mu_h S_h^i + \omega R_h^i) + \theta(\Lambda_h - \frac{b\beta_h S_h^{i+1} I_m^i}{1+\nu_h I_m^i} - \mu_h S_h^{i+1} + \omega R_h^i) \\ \frac{E_h^{i+1}-E_h^i}{\Phi(\Delta t)} = (1-\theta)(\frac{b\beta_h S_h^i I_m^i}{1+\nu_h I_m^i} - (\alpha_h+\mu_h)E_h^i) + \theta(\frac{b\beta_h S_h^{i+1} I_m^i}{1+\nu_h I_m^i} - (\alpha_h+\mu_h)E_h^{i+1}) \\ \frac{I_h^{i+1}-I_h^i}{\Phi(\Delta t)} = (1-\theta)(\alpha_h E_h^i - (r+\mu_h+\delta_h)I_h^i) + \theta(\alpha_h E_h^{i+1} - (r+\mu_h+\delta_h)I_h^{i+1}) \\ \frac{R_h^{i+1}-R_h^i}{\Phi(\Delta t)} = (1-\theta)(rI_h^i - (\mu_h+\omega)R_h^i) + \theta(rI_h^{i+1} - \mu_h R_h^{i+1} - \omega R_h^i) \\ \frac{S_m^{i+1}-S_m^i}{\Phi(\Delta t)} = (1-\theta)(\Lambda_m - \frac{b\beta_m S_m^i I_h^i}{1+\nu_m I_h^i} - \mu_m S_m^i) + \theta(\Lambda_m - \frac{b\beta_m S_m^{i+1} I_h^{i+1}}{1+\nu_m I_h^{i+1}} - \mu_m S_m^{i+1}) \\ \frac{E_m^{i+1}-E_m^i}{\Phi(\Delta t)} = (1-\theta)(\frac{b\beta_m S_m^i I_h^i}{1+\nu_m I_h^i} - (\alpha_m+\mu_m)E_m^i) + \theta(\frac{b\beta_m S_m^{i+1} I_h^{i+1}}{1+\nu_m I_h^{i+1}} - (\alpha_m+\mu_m)E_m^{i+1}) \\ \frac{I_m^{i+1}-I_m^i}{\Phi(\Delta t)} = (1-\theta)(\alpha_m E_m^i - (\mu_m+\delta_m)I_m^i) + \theta(\alpha_m E_m^{i+1} - (\mu_m+\delta_m)I_m^{i+1}). \end{cases} \tag{17}$$

Here $S_h^i \approx S_h(t_i)$ and it is analogous for the other components. The discrete model (17) can be written as follows.

$$S_h^{i+1}\left(1+\Phi(\Delta t)\theta\left(\frac{b\beta_h I_m^i}{1+\nu_h I_m^i}+\mu_h\right)\right) = S_h^i + \Phi(\Delta t)\left((1-\theta)\left(-\frac{b\beta_h S_h^i I_m^i}{1+\nu_h I_m^i} - \mu_h S_h^i\right) + \Lambda_h + \omega R_h^i\right), \tag{18}$$

$$E_h^{i+1}(1+\Phi(\Delta t)\theta(\alpha_h+\mu_h)) = E_h^i + \Phi(\Delta t)\left((1-\theta)\left(\frac{b\beta_h S_h^i I_m^i}{1+\nu_h I_m^i} - (\alpha_h+\mu_h)E_h^i\right) + \theta\frac{b\beta_h S_h^{i+1} I_m^i}{1+\nu_h I_m^i}\right), \tag{19}$$

$$I_h^{i+1}(1+\Phi(\Delta t)\theta(r+\mu_h+\delta_h)) = I_h^i + \Phi(\Delta t)((1-\theta)(\alpha_h E_h^i - (r+\mu_h+\delta_h)I_h^i) + \theta\alpha_h E_h^{i+1}), \tag{20}$$

$$R_h^{i+1}(1+\Phi(\Delta t)\theta\mu_h) = R_h^i + \Phi(\Delta t)((1-\theta)(rI_h^i - \mu_h R_h^i) + \theta rI_h^{i+1} - \omega R_h^i), \tag{21}$$

$$S_m^{i+1}\left(1+\Phi(\Delta t)\theta\left(\frac{b\beta_m I_h^{i+1}}{1+\nu_m I_h^{i+1}}+\mu_m\right)\right) = S_m^i + \Phi(\Delta t)\left((1-\theta)\left(-\frac{b\beta_m S_m^i I_h^i}{1+\nu_m I_h^i} - \mu_m S_m^i\right) + \Lambda_m\right), \tag{22}$$

$$E_m^{i+1}(1+\Phi(\Delta t)\theta(\alpha_m+\mu_m)) = E_m^i + \Phi(\Delta t)\left((1-\theta)\left(\frac{b\beta_m S_m^i I_h^i}{1+\nu_m I_h^i} - (\alpha_m+\mu_m)E_m^i\right) + \theta\frac{b\beta_m S_m^{i+1} I_h^{i+1}}{1+\nu_m I_h^{i+1}}\right), \tag{23}$$

$$I_m^{i+1}(1+\Phi(\Delta t)\theta(\mu_m+\delta_m)) = I_m^i + \Phi(\Delta t)((1-\theta)(\alpha_m E_m^i - (\mu_m+\delta_m)I_m^i) + \theta\alpha_m E_m^{i+1}). \tag{24}$$

Remark 1. Clearly, the system (17) is an implicit scheme. However, its realization is effective, since for each components the approximation on the new time-level can be defined by solving a linear system with simple (tridiagonal) matrix.

Remark 2. We note that the discrete model (17) can be obtained by using some special sequential splitting when the right hand is split into two parts by θ and $1-\theta$, and we apply the explicit and implicit Euler methods to the sub-problems.

Remark 3. By a usual computation one can easily derive that the local error of the scheme (17) is $O(\Delta t)$ for any θ.

In the following, we analyze model (17) qualitatively.

3.3. Positivity preservation property

Let $u(t) = (S_h(t),\ E_h(t),\ I_h(t),\ R_h(t),\ S_m(t),\ E_m(t),\ I_m(t))^T$ be the exact solution of the system (5). For $u(t)$ the following properties are valid, the intervals $(0,\ \frac{\Lambda_h}{\mu_h}]$ and $(0,\ \frac{\Lambda_m}{\mu_m}]$ are positively invariant for the total populations (both humans and mosquitoes) and its each component for humans and mosquitoes, respectively [5].

We denote by $u^i = (S_h^i,\ E_h^i,\ I_h^i,\ R_h^i,\ S_m^i,\ E_m^i,\ I_m^i)^T$ the approximation to $u(t)$ at the time point $t = t_i$. To preserve the positively invariant property numerically, we need to guarantee that if the total populations and each component of u^i in the system (17) are on the intervals $(0,\ \frac{\Lambda_h}{\mu_h}]$ and $(0,\ \frac{\Lambda_m}{\mu_m}]$ for humans and mosquitoes, respectively, then the same property is valid for u^{i+1}. Firstly, we investigate the lower bound of the intervals, i.e., positivity preserving property.

According to the first equation of the system (17), the solution S_h^{i+1} is positive if and only if the right side of (18) is positive. Thus, we can get a sufficient and necessary condition

$$S_h^i\left(1-\Phi(\Delta t)(1-\theta)\left(\frac{b\beta_h I_m^i}{1+\nu_h I_m^i}+\mu_h\right)\right) + \Phi(\Delta t)t(\Lambda_h+\omega R_h^i) > 0\,. \tag{25}$$

This is equivalent to

$$S_h^i > \Phi(\Delta t)\left(S_h^i(1-\theta)\left(\frac{b\beta_h I_m^i}{1+\nu_h I_m^i}+\mu_h\right) - (\Lambda_h+\omega R_h^i)\right). \tag{26}$$

It is easy to see that if the multiplier of $\Phi(\Delta t)$ is non-positive, then the inequality is valid. If it is positive, which can be translated to a positive lower bound for S_h^i, then it is equivalent to

$$\Phi(\Delta t) < \frac{S_h^i}{S_h^i(1-\theta)\left(\frac{b\beta_h I_m^i}{1+\nu_h I_m^i}+\mu_h\right)-(\Lambda_h+\omega R_h^i)}. \tag{27}$$

Since $S_h^i \in (0, \frac{\Lambda_h}{\mu_h}]$ and $I_m^i \in (0, \frac{\Lambda_m}{\mu_m}]$, elementary calculation gives that

$$\frac{\frac{\Lambda_h}{\mu_h}}{\frac{\Lambda_h}{\mu_h}(1-\theta)\left(\frac{b\beta_h \frac{\Lambda_m}{\mu_m}}{1+\nu_h \frac{\Lambda_m}{\mu_m}}+\mu_h\right)-(\Lambda_h+0)} < \frac{S_h^i}{S_h^i(1-\theta)\left(\frac{b\beta_h I_m^i}{1+\nu_h I_m^i}+\mu_h\right)-(\Lambda_h+\omega R_h^i)}. \tag{28}$$

It implies that if

$$\Phi(\Delta t) < \frac{\mu_m+\nu_h\Lambda_m}{(1-\theta)b\beta_h\Lambda_m-\theta\mu_h(\mu_m+\nu_h\Lambda_m)}, \tag{29}$$

then the solution S_h^{i+1} is positive. The second equation of the system (17) results in E_h^{i+1} is positive provided that

$$E_h^i-\Phi(\Delta t)(E_h^i(1-\theta)(\alpha_h+\mu_h)-(1-\theta)\frac{b\beta_h S_h^i I_m^i}{1+\nu_h I_m^i}-\theta\frac{b\beta_h S_h^{i+1} I_m^i}{1+\nu_h I_m^i})>0. \tag{30}$$

If the multiplier of $\Phi(\Delta t)$ is non-positive, then E_h^{i+1} is positive unconditionally. Otherwise, E_h^{i+1} is positive as long as

$$\Phi(\Delta t) < \frac{E_h^i}{E_h^i(1-\theta)(\alpha_h+\mu_h)-(1-\theta)\frac{b\beta_h S_h^i I_m^i}{1+\nu_h I_m^i}-\theta\frac{b\beta_h S_h^{i+1} I_m^i}{1+\nu_h I_m^i}}. \tag{31}$$

Clearly,

$$\frac{E_h^i}{E_h^i(1-\theta)(\alpha_h+\mu_h)} < \frac{E_h^i}{E_h^i(1-\theta)(\alpha_h+\mu_h)-(1-\theta)\frac{b\beta_h S_h^i I_m^i}{1+\nu_h I_m^i}-\theta\frac{b\beta_h S_h^{i+1} I_m^i}{1+\nu_h I_m^i}}. \tag{32}$$

If

$$\Phi(\Delta t) < \frac{1}{(1-\theta)(\alpha_h+\mu_h)}, \tag{33}$$

then E_h^{i+1} is positive. Similar calculation is valid for the other components and hence our results are summarized in the following lemma.

Lemma 1. *Suppose Λ_h, $\Lambda_m > 0$, the initial data of the system (17), and the initial total populations are on the intervals $(0, \frac{\Lambda_h}{\mu_h}]$ and $(0, \frac{\Lambda_m}{\mu_m}]$, respectively. If the step-size function $\Phi(\Delta t) \in (0, h^*(\theta)]$, then the solution of the system (17) is positive. Where*

$$h^*(\theta) = \begin{cases} \frac{1}{1-\theta} min\{h_1, h_2\} & \theta \neq 1 \\ \frac{1}{\omega} & \theta = 1, \end{cases} \tag{34}$$

with

$$A_1 = \frac{\mu_m+\nu_h\Lambda_m}{b\beta_h\Lambda_m-\frac{\theta}{1-\theta}\mu_h(\mu_m+\nu_h\Lambda_m)} \quad A_2 = \frac{\mu_m+\nu_h\Lambda_m}{b\beta_h\Lambda_m-\frac{\theta}{1-\theta}\mu_h(\mu_m+\nu_h\Lambda_m)},$$

$$B_1 = \min\left\{\frac{1}{\alpha_h+\mu_h}, \frac{1}{r+\mu_h+\delta_h}, \frac{1}{\mu_h+\frac{\omega}{1-\theta}}\right\} \quad and \quad B_2 = \min\left\{\frac{1}{\alpha_m+\mu_m}, \frac{1}{\mu_m+\delta_m}\right\}.$$

- *If $A_1 > 0$, then $h_1 = \min\{A_1, B_1\}$, otherwise $h_1 = B_1$.*
- *If $A_2 > 0$, then $h_2 = \min\{A_2, B_2\}$, otherwise $h_2 = B_2$.*

Remark 4. Note if the fractions A_1 and A_2 are negative, then S_h^{i+1} and S_m^{i+1} are positive unconditionally for the step size Δt, respectively.

3.4. Total populations, upper bound, and positively invariant property

In this part, we prove the upper bound of the solution and total populations of the discrete model (17) and invariance property for some sets.

According to (7), the number of the total population at time t_{i+1} for humans in the discrete model (17) is defined as

$$V_h^{i+1} = S_h^{i+1} + E_h^{i+1} + I_h^{i+1} + R_h^{i+1}. \tag{35}$$

By summing up the first four equations of the system (17) and regarding (35) we attain

$$V_h^{i+1}(1 + \Phi(\Delta t)\theta\mu_h) = V_h^i + \Phi(\Delta t)(\Lambda_h - (1-\theta)\mu_h V_h^i - (1-\theta)\delta_h I_h^i - \theta\delta_h I_h^{i+1}) \tag{36}$$

for $\theta \in [0, 1]$. Based on Lemma 1, we know that under the condition $\Phi(\Delta t) \in (0, h^*(\theta)]$ the value of V_h^{i+1} is positive. From (36) we have

$$V_h^{i+1}(1 + \Phi(\Delta t)\theta\mu_h) \le V_h^i(1 - \Phi(\Delta t)(1-\theta)\mu_h) + \Phi(\Delta t)\Lambda_h. \tag{37}$$

If

$$V_h^i \le \frac{\Lambda_h}{\mu_h}, \tag{38}$$

then for the right side of (37) we have

$$V_h^i(1 - \Phi(\Delta t)(1-\theta)\mu_h) + \Phi(\Delta t)\Lambda_h \le \frac{\Lambda_h}{\mu_h}(1 - \Phi(\Delta t)(1-\theta)\mu_h) + \Phi(\Delta t)\Lambda_h. \tag{39}$$

Consequently,

$$V_h^{i+1} \le \frac{\Lambda_h}{\mu_h}. \tag{40}$$

Hence $V_h^0 \le \frac{\Lambda_h}{\mu_h}$ implies the interval $(0, \frac{\Lambda_h}{\mu_h}]$ is positively invariant for the total population of humans. The same result is valid for mosquitoes. Hence, the following statement is proven.

Theorem 1. *Suppose Λ_h, $\Lambda_m > 0$, the initial data of the system (17), and the initial total populations are on the intervals $(0, \frac{\Lambda_h}{\mu_h}]$ and $(0, \frac{\Lambda_m}{\mu_m}]$, respectively, then for the step-size function $\Phi(\Delta t) \in (0, h^*(\theta)]$, the intervals $(0, \frac{\Lambda_h}{\mu_h}]$ and $(0, \frac{\Lambda_m}{\mu_m}]$ are positively invariant for the total populations for humans and mosquitoes, respectively.*

Corollary 1. *Under the conditions of Theorem 1, the intervals $(0, \frac{\Lambda_h}{\mu_h}]$ and $(0, \frac{\Lambda_m}{\mu_m}]$ are positively invariant for each component of the solution of the system (17) for humans and mosquitoes, respectively.*

In the sequel, we consider the case when the numbers of the initial populations are greater than $\frac{\Lambda_h}{\mu_h}$ and $\frac{\Lambda_m}{\mu_m}$ for humans and mosquitoes, respectively. For this case, which is shown in [5] the intervals $(0, V_h^*)$ and $(0, V_m^*)$ are positively invariant for the total populations and each component of the solution of the extended Ross model (5) for humans and mosquitoes, respectively, where the notations

$$V_h^* = \max\left\{V_h(0), \frac{\Lambda_h}{\mu_h}\right\}, \tag{41}$$

and

$$V_m^* = \max\left\{V_m(0), \frac{\Lambda_m}{\mu_m}\right\} \tag{42}$$

are used. We can demonstrate that this property is valid for the discrete model (17).

Theorem 2. *Assume that $\Lambda_h, \Lambda_m > 0$, the initial data of the system (17) and initial total populations are on the intervals $(0, V_h^*)$ and $(0, V_m^*)$, respectively. Then the intervals $(0, V_h^*)$ and $(0, V_m^*)$ are positively invariant for the total populations and each component of the solution of the system (17) for humans and mosquitoes respectively for the step-size function $\Phi(\Delta t) \in (0, h^{**}(\theta)]$. Here*

$$h^{**}(\theta) = \begin{cases} \frac{1}{1-\theta} min\{h_1^*, h_2^*\} & \theta \ne 1 \\ \frac{1}{\omega} & \theta = 1, \end{cases} \tag{43}$$

with

$$A_1^* = \frac{V_h^*(1 + \nu_h V_m^*)}{V_h^*(b\beta_h V_m^* + \mu_h(1 + \nu_h V_m^*)) - \frac{\Lambda_h(1+\nu_h V_m^*)}{1-\theta}}$$

$$A_2^* = \frac{V_h^*(1+\nu_h V_m^*)}{V_h^*(b\beta_h V_m^* + \mu_h(1+\nu_h V_m^*)) - \frac{\Lambda_h(1+\nu_h V_m^*)}{1-\theta}},$$

$$B_1^* = \min\left\{\frac{1}{\alpha_h+\mu_h}, \frac{1}{r+\mu_h+\delta_h}, \frac{1}{\mu_h+\frac{\omega}{1-\theta}}\right\} \quad \text{and} \quad B_2^* = \min\left\{\frac{1}{\alpha_m+\mu_m}, \frac{1}{\mu_m+\delta_m}\right\}.$$

- *If* $A_1^* > 0$, *then* $h_1^* = \min\{A_1^*, B_1^*\}$, *otherwise* $h_1^* = B_1^*$.
- *If* $A_2^* > 0$, *then* $h_2^* = \min\{A_2^*, B_2^*\}$, *otherwise* $h_2^* = B_2^*$.

Proof. Firstly, to prove the lower bound, positivity preservation property, we follow the proof of Lemma 1, i.e., if the initial data of the system (17) are on the intervals $(0, V_h^*)$ and $(0, V_m^*)$ respectively, then the right side of the first equation of the system (17) is positive if the multiplier of $\Phi(\Delta t)$ of the Eq. (26) is non-positive. Otherwise, from relation (27), $S_h^i \in (0, V_h^*)$, and $I_m^i \in (0, V_m^*)$ we obtain

$$\Phi(\Delta t) \le \frac{V_h^*(1+\nu_h V_m^*)}{(1-\theta)V_h^*(b\beta_h V_m^* + \mu_h(1+\nu_h V_m^*)) - \Lambda_h(1+\nu_h V_m^*)}. \tag{44}$$

We have the analogous calculation for other components. In the sequel, we prove the upper bound when the initial total populations are greater than $\frac{\Lambda_h}{\mu_h}$ and $\frac{\Lambda_m}{\mu_m}$, respectively.

According to the number of the total population for humans at t_{i+1} defined in (35) and the first part of the present proof, the value of V_h^{i+1} is positive for any step-size function $\Phi(\Delta t) \in (0, h^{**}(\theta)]$. Then under the assumption $V_h^i > \frac{\Lambda_h}{\mu_h}$ and from (37) we obtain

$$V_h^{i+1}(1+\Phi(\Delta t)\theta\mu_h) < V_h^i(1-\Phi(\Delta t)(1-\theta)\mu_h) + \Phi(\Delta t)\mu_h) \tag{45}$$

for $\theta \in [0,1]$. Hence,

$$V_h^{i+1} < V_h^i, \tag{46}$$

implying the sequence of the solutions is decreasing and we have

$$V_h^{i+1} < V_h^0. \tag{47}$$

Also, based on Theorem 1, we prove the upper bound when $V_h^0 \le \frac{\Lambda_h}{\mu_h}$, the interval $(0, V_h^*)$ is positively invariant for the total population of humans. A similar result is valid for mosquitoes. □

Remark 5. In this remark, particularly the boundedness of V_h^i is indicated., i.e., the statement of the limit behavior of Theorem 2. We assume that $V_h^i > \frac{\Lambda_h}{\mu_h}$, then for $\theta \in [0,1]$ relation (37) yields

$$V_h^{i+1}(1+\Phi(\Delta t)\theta\mu_h) < V_h^i(1-\Phi(\Delta t)(1-\theta)\mu_h + \Phi(\Delta t)\mu_h). \tag{48}$$

Hence,

$$V_h^{i+1} < V_h^i. \tag{49}$$

This means that the positive sequence $\{V_h^i\}$ is decreasing,

$$V_h^i < V_h(0), \tag{50}$$

and as a result it converges. i.e.,

$$\lim_{i\to\infty} V_h^i = \widetilde{V} \tag{51}$$

Then from (37) and (51) we obtain

$$\widetilde{V}(1+\Phi(\Delta t)\theta\mu_h) \le \widetilde{V}(1-\Phi(\Delta t)(1-\theta)\mu_h) + \Phi(\Delta t)\Lambda_h. \tag{52}$$

Consequently,

$$\widetilde{V} \le \frac{\Lambda_h}{\mu_h}. \tag{53}$$

It means that if the initial total number of the humans population $V_h(0) > \frac{\Lambda_h}{\mu_h}$, then the total number of the population decreases to the interval $(0, \frac{\Lambda_h}{\mu_h}]$. The same result is valid for mosquitoes.

Remark 6. If $\Lambda_h = 0$, then from (37) we obtain

$$V_h^{i+1}(1+\Phi(\Delta t)\theta\mu_h) \le V_h^i(1-\Phi(\Delta t)(1-\theta)\mu_h), \tag{54}$$

implying

$$V_h^{i+1} \leq V_h^i \left(1 - \frac{\Phi(\Delta t)\mu_h}{1 + \Phi(\Delta t)\theta\mu_h}\right). \tag{55}$$

It denotes the positive sequence $\{V_h^i\}$ is decreasing, and it is convergent. i.e.,

$$\lim_{i \to +\infty} V_h^i = \overline{V}. \tag{56}$$

Moreover,

$$V_h^i \leq V_h(0). \tag{57}$$

From (54) and (56) we attain

$$\overline{V}(1 + \Phi(\Delta t)\theta\mu_h)) \leq \overline{V}(1 - \Phi(\Delta t)(1-\theta)\mu_h), \tag{58}$$

yielding

$$\overline{V} \leq 0. \tag{59}$$

Since V_h^i is positive, $\overline{V} \geq 0$ in (56). Hence, due to (59), we obtain $\overline{V} = 0$. This means that in the absence of the birth but with the existence of natural death, the total number of the population tends to zero.

Remark 7. When there is no death and birth, i.e., in the model $\Lambda_h = \mu_h = \delta_h = 0$, then obviously $V_h^{i+1} = V_h^i$. Therefore, the total number of the population in the discrete model is $V_h^i = V_h(0)$=constant for any i. This is in complete agreement with the natural expectation of the model.

3.5. Domain of the step-size functions

In this part, we seek the suitable domain for the step-size functions discussed in the Section 3.1 in such a way $\Phi(\Delta t) \in (0, h^*(\theta)]$.

- The function $\Phi(\Delta t) = \Delta t$ is the identity function and clearly, for $\Delta t \in (0, h^*(\theta)]$ the intervals $(0, \frac{\Lambda_h}{\mu_h}]$ and $(0, \frac{\Lambda_m}{\mu_m}]$ are positively invariant
  for the total populations and each component of the solution for humans and mosquitoes, respectively.
- Regarding the step-size function $\Phi_C(\Delta t)$ (16), we seek a suitable $C > 0$ for the fixed step size Δt, denoted by the step-size function

$$\Psi_{\Delta t}(C) = \begin{cases} \frac{1-e^{-C\Delta t}}{C}, & \text{for } C \neq 0, \\ 0, & \text{for } C = 0. \end{cases} \tag{60}$$

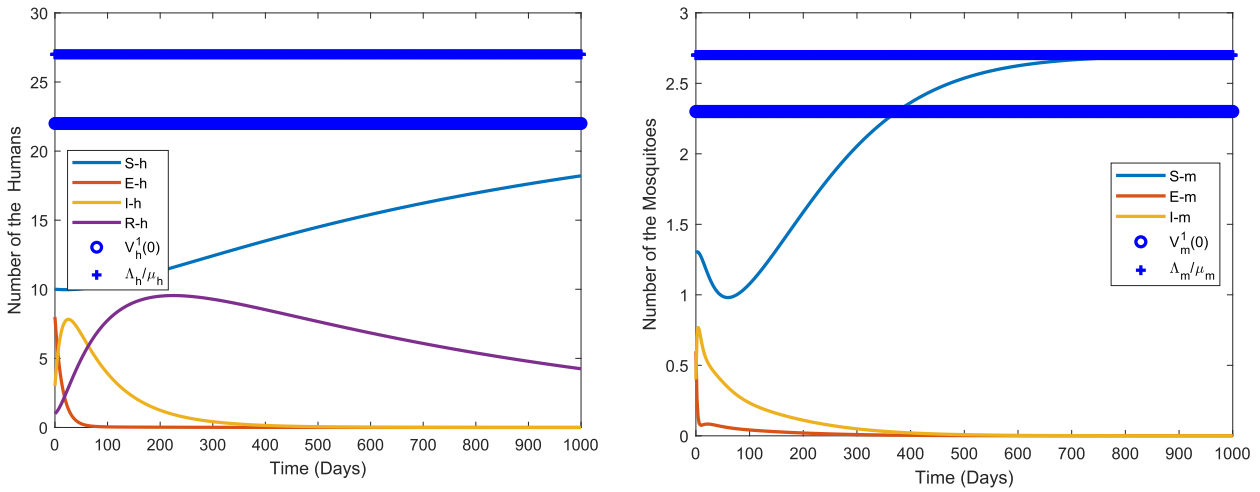

(a) Human (b) Mosquito

Fig. 1. $\Phi(\Delta t) = \Delta t$, Explicit Euler Method ($\theta = 0$), Δt=2.

Note the functions $\Phi_C(\Delta t)$ and $\Psi_{\Delta t}(C)$ are substantially the same. The function $\Phi_C(\Delta t)$ (16) concentrates on variable Δt with the fixed C, while the function $\Psi_{\Delta t}(C)$ focuses on variable C with the fixed step sizes Δt. The step-size function (60) with any $C > 0$ is monotonically decreasing, and the conditions (13) and (14) are satisfied. We covenant

$$\Psi_{\Delta t}(0) = 0. \tag{61}$$

Since $\lim_{C\to+\infty} \Psi_{\Delta t}(C) = 0$ and $\sup \Psi_{\Delta t}(C) = \Delta t$, we obtain if

1. $\Delta t < h^*(\theta)$, then $\Psi_{\Delta t}(C) \in (0, h^*(\theta)]$ for all $C > 0$.
2. $\Delta t \geq h^*(\theta)$, there exists C_0 such that $\Psi_{\Delta t}(C) \in (0, h^*(\theta)]$ for $C \geq C_0$.

Here C_0 is the solution of

$$e^{-C_0\Delta t} + C_0 h^*(\theta) - 1 = 0, \tag{62}$$

implying the choice

$$C_0 \geq \frac{1}{h^*(\theta)} \tag{63}$$

is a sufficient condition for the suitable choice of the parameter C_0.

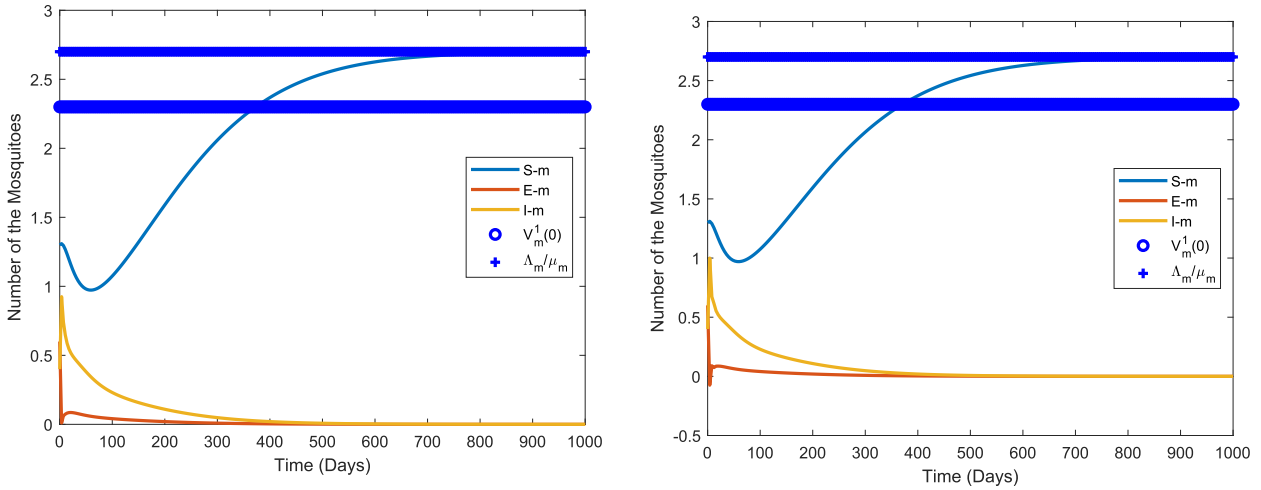

(a) Δt=3.5 (b) Δt=4

Fig. 2. $\Phi(\Delta t) = \Delta t$, Explicit Euler Method ($\theta = 0$), Mosquitoes.

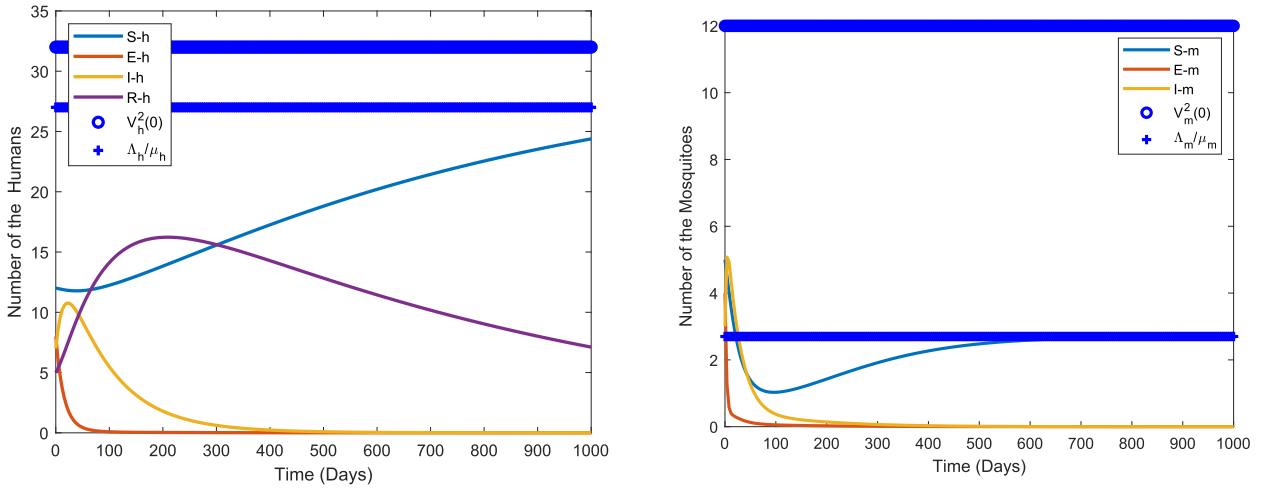

(a) Human (b) Mosquito

Fig. 3. $\Phi(\Delta t) = \Delta t$, Semi-Trapezoidal Method ($\theta = 0.5$), Δt=4.

Remark 8. The exact solution of Eq. (62) lies on the principal branch of the Lambert W function as

$$C_0 = \frac{HW_0(\frac{-\Delta t}{H}e^{\frac{-\Delta t}{H}}) + \Delta t}{H\Delta t} \tag{64}$$

for $\Delta t \geq H$.

- The step-size function (60) with $C < 0$ is equivalent to the function

$$\Psi_{\Delta t}(C) = \frac{e^{C\Delta t} - 1}{C}, \tag{65}$$

with $C > 0$. Since the function (65) is monotonically increasing function with the property

$$\lim_{C \to +\infty} \Psi_{\Delta t}(C) = +\infty, \tag{66}$$

we obtain if

1. $\Delta t \leq h^*(\theta)$, then there exists C_0 such that $\Psi_{\Delta t}(C) \in (0, h^*(\theta)]$ for all $C \leq C_0$.
2. $\Delta t > h^*(\theta)$, then there is no C such that $\Psi_{\Delta t}(C) \in (0, h^*(\theta)]$.

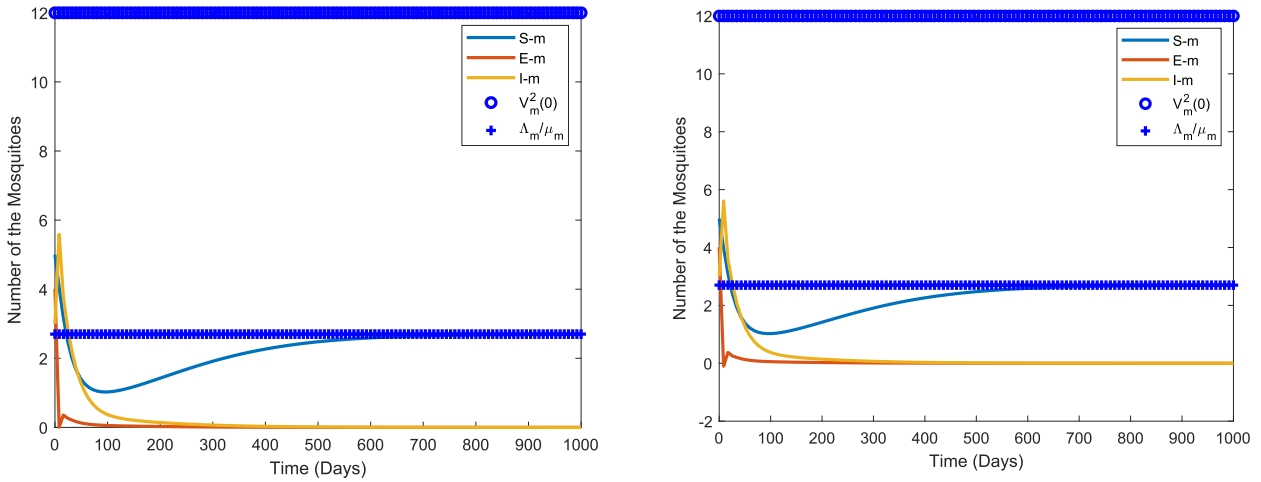

(a) Δt=8 (b) Δt=8.5

Fig. 4. $\Phi(\Delta t) = \Delta t$, Semi-Trapezoidal Method ($\theta = 0.5$), Mosquitoes.

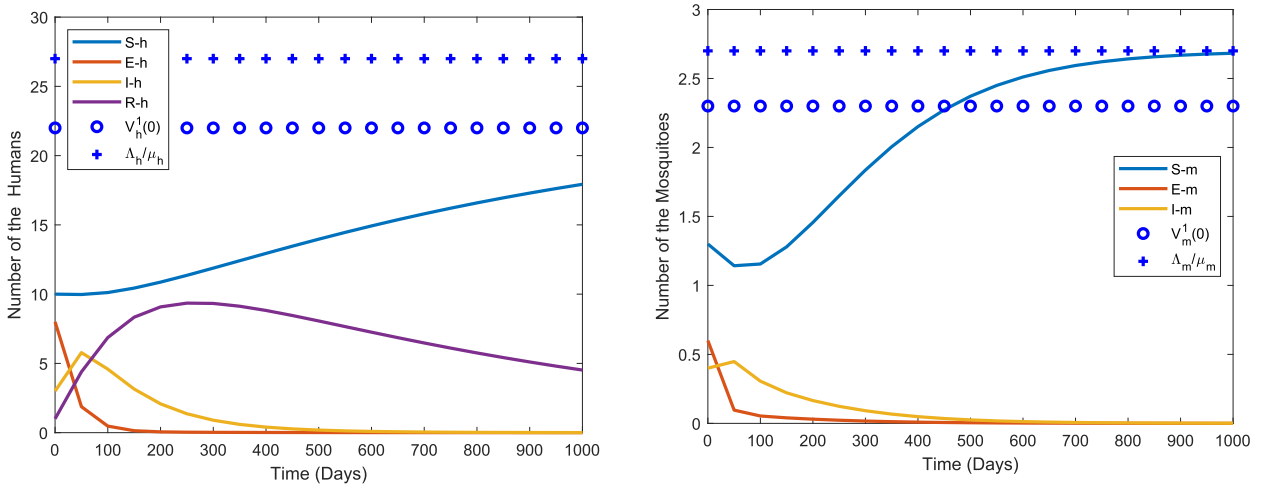

(a) Human (b) Mosquito

Fig. 5. $\Phi(\Delta t) = \Delta t$, Semi-Implicit Euler Method ($\theta = 1$), $\Delta t = 50$.

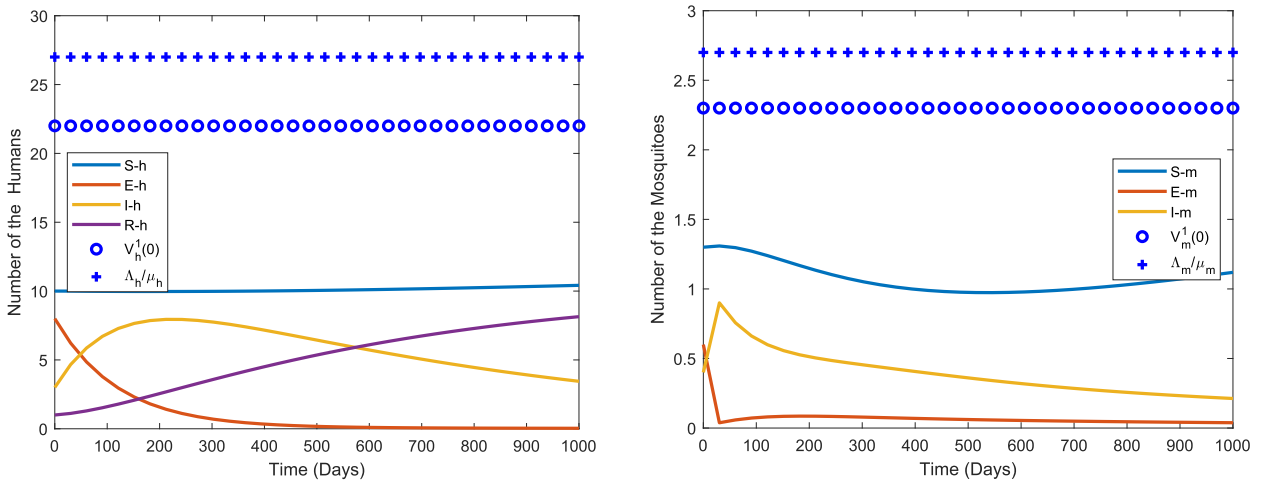

(a) Human (b) Mosquito

Fig. 6. $\Psi_{30}(\frac{1}{h^*(0)})$, Explicit Euler Method ($\theta = 0$).

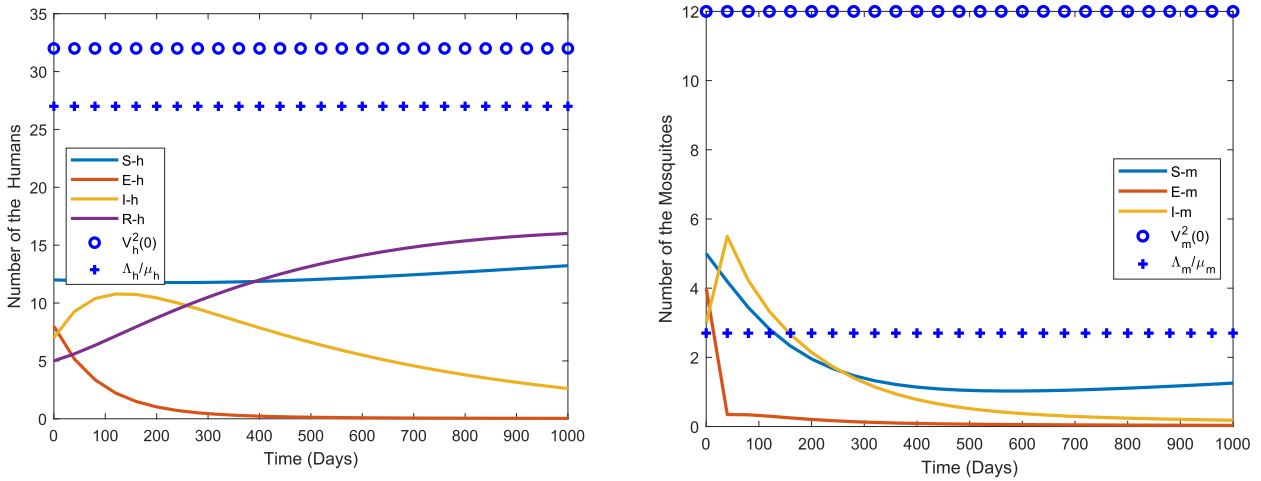

(a) Human (b) Mosquito

Fig. 7. $\Psi_{40}(\frac{1}{h^*(0.5)})$, Semi-Trapezoidal Method ($\theta = 0.5$).

Table 1
Values of the parameters for the numerical results.

$S_h^1(0) = 10$	$E_h^1(0) = 8$	$I_h^1(0) = 3$	$R_h^1(0) = 1$
$S_m^1(0) = 1.3$	$E_m^1(0) = 0.6$	$I_m^1(0) = 0.4$	
$S_h^2(0) = 12$	$E_h^2(0) = 8$	$I_h^2(0) = 7$	$R_h^2(0) = 5$
$S_m^2(0) = 5$	$E_m^2(0) = 4$	$I_m^2(0) = 3$	
$\Lambda_h = 0.0027$	$\Lambda_m = 0.027$	$\beta_h = 0.1$	$\beta_m = 0.3$
$\mu_h = 0.0001$	$\mu_m = 0.010$	$\delta_h = 0.2 \times 10^{-4}$	$\delta_m = 0.05$
$\alpha_h = 0.067$	$\alpha_m = 0.29$	$r = 0.012$	$\omega = 0.0011$
$\nu_h = 0.5$	$\nu_m = 0.01$	b=0.01	
$V_h^1(0) = 22$	$\frac{\Lambda_h}{\mu_h} = 27$	$V_m^1(0) = 2.3$	$\frac{\Lambda_m}{\mu_m} = 2.7$
$V_h^2(0) = 32$		$V_m^2(0) = 12$	

Remark 9. The exact solution for the function (65) is on the negative branch of the Lambert W function as

$$C_0 = \frac{-HW_{-1}(\frac{-\Delta t}{H}e^{\frac{-\Delta t}{H}}) - \Delta t}{H\Delta t}. \tag{67}$$

4. Numerical simulations

In this section, we give some numerical examples to verify the theoretical results obtained in Section 3. We investigate the sharpness of the upper bounds $h^*(\theta)$ and $h^{**}(\theta)$ and positively invariant property for the intervals $(0, \frac{\Lambda_h}{\mu_h}]$, $(0, \frac{\Lambda_m}{\mu_m}]$, $(0, V_h^*)$, and $(0, V_m^*)$ for the total populations and each component of the solution for humans and mosquitoes, respectively at any time. The applied parameters and initial data are defined from the literature and they are given in Table 1 [3,4,20].

Figure 1 visualizes the validity of Theorem 1 and Corollary 1 for the standard explicit Euler method, ($\theta = 0$). Figure 1(a)-(b) denote the intervals $(0, \frac{\Lambda_h}{\mu_h}]$ and $(0, \frac{\Lambda_m}{\mu_m}]$ are positively invariant for each component of the solution of the system (17) for humans and mosquitoes, respectively when $\Delta t \in (0, h^*(0)]$, $h^*(0) = 3.33$. Figure 2 depicts the results when $\Delta t > h^*(0)$,

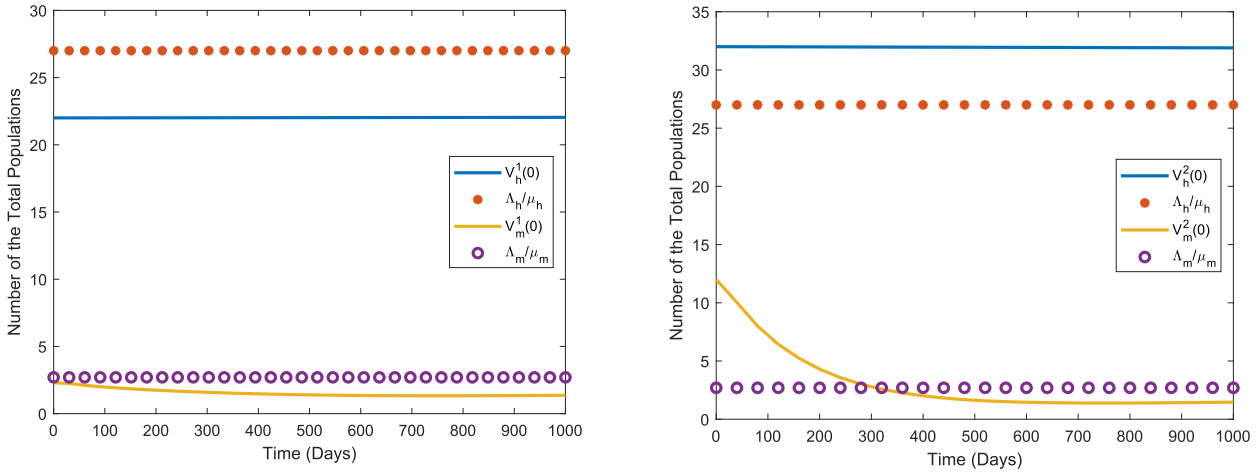

(a) Explicit Euler Method, $\Psi_{30}(\frac{1}{h^*(0)})$ (b) Semi-Trapezoidal Method, $\Psi_{40}(\frac{1}{h^{**}(0.5)})$

Fig. 8. Number of the Total Population for Humans and Mosquitoes.

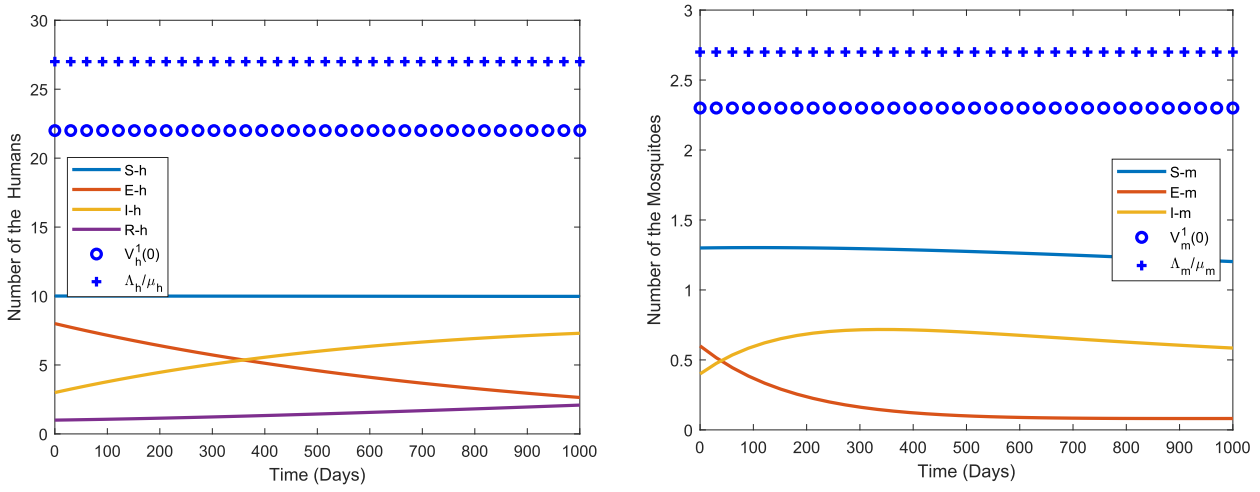

(a) Humans (b) Mosquitoes

Fig. 9. $\Psi_{30}(2)$, Explicit Euler Method ($\theta = 0$).

i.e., $\Delta t \notin (0, h^*(0)]$. In Fig. 2(a) the positively invariant property of the intervals $(0, \frac{\Lambda_h}{\mu_h}]$ and $(0, \frac{\Lambda_m}{\mu_m}]$ is preserved for each component of the solution stating the step size tolerance $h^*(0)$ is a sufficient condition, while in Fig. 2(b) this property is not preserved. Figures 1 and 2 show the sharpness of the sufficient condition for the step size Δt and they illustrate the solution does not exceed the upper bounds when the time interval is sufficiently large. This example illustrates the behavior of the system (17) for the standard semi-trapezoidal method, $\theta = 0.5$, when $\Delta t \in (0, h^{**}(0.5)]$, here $h^{**}(0.5) = 6.66$. The intervals $(0, V_h^*)$ and $(0, V_m^*)$ are positively invariant for each component of the solution of the system (17) for humans and mosquitoes, respectively. Figure 4 shows the step size tolerance $h^{**}(0.5)$ is a sufficient condition for the standard semi-trapezoidal method. In Fig. 4(a), the interval $(0, V_m^*)$ is positively invariant for each component of the solution for mosquitoes with the semi-trapezoidal method for $\Delta t \notin (0, h^{**}(0.5)]$ whereas Fig. 4(b) indicates this property does not hold for $\Delta t \notin (0, h^{**}(0.5)]$. Figures 3 and 4 consider the results of Theorem 2. Figure 5 visualizes the intervals $(0, \frac{\Lambda_h}{\mu_h}]$ and $(0, \frac{\Lambda_m}{\mu_m}]$ are positively invariant for each component of the solution of the system (17) with the standard semi-implicit Euler method, $\theta = 1$, for the adequately large step size. For this method $h^*(1) = 100$. Figure 6 verifies the validity of Theorem 1 and Corollary 1 with the step-size function (60) applied to the explicit Euler method for sufficiently large step size, $\Delta t = 30$, for humans and mosquitoes. In Fig. 7, the intervals $(0, V_h^*)$ and $(0, V_m^*)$ are positively invariant for each component of the solution for

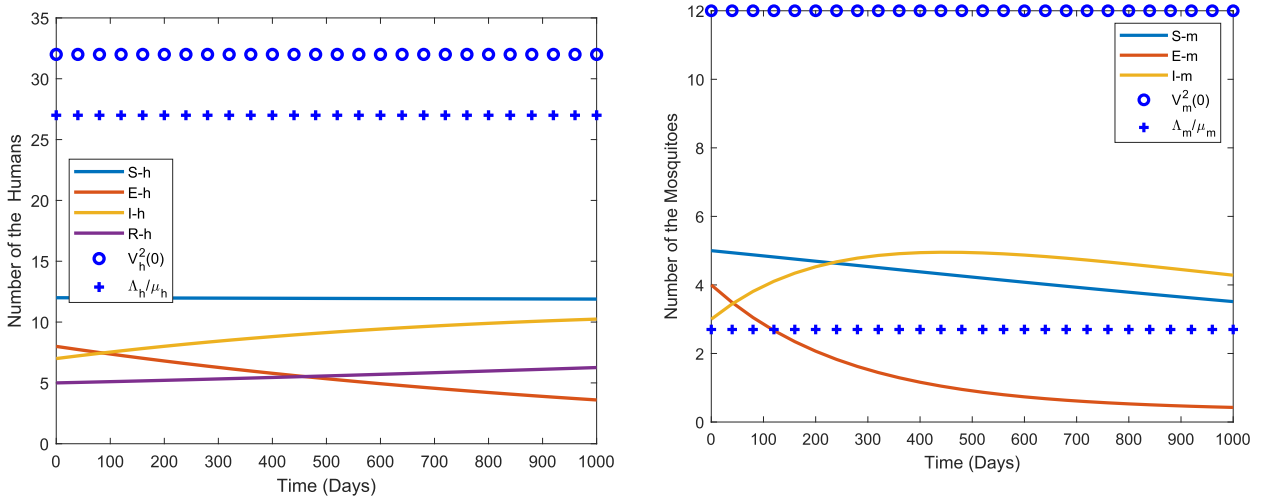

(a) Humans (b) Mosquitoes

Fig. 10. $\Psi_{40}(2)$, Semi-Trapezoidal Method ($\theta = 0.5$).

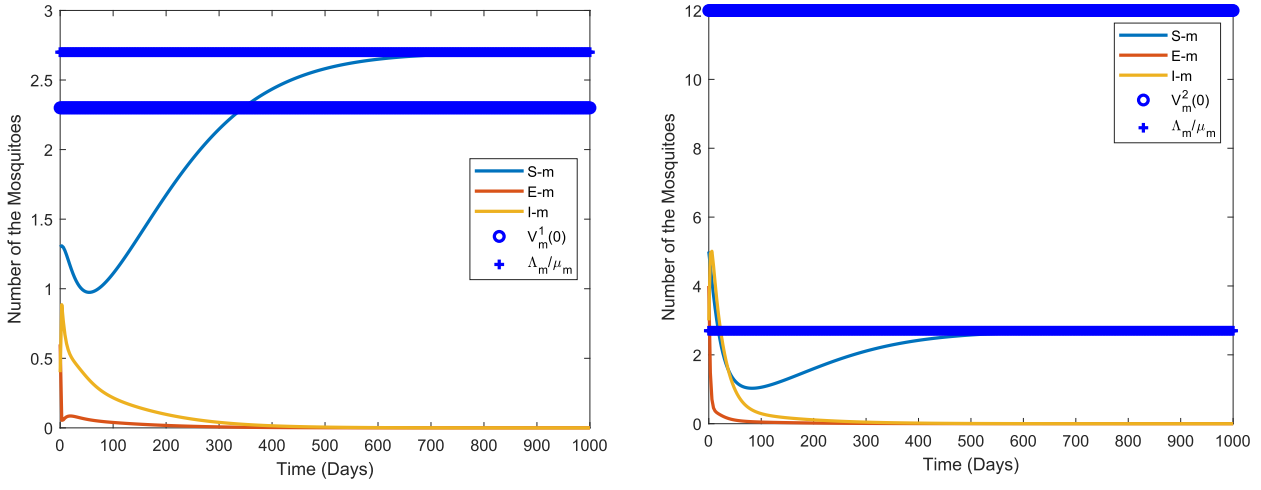

(a) $\Psi_3(0.05)$, Explicit Euler Method (b) $\Psi_3(0.1)$, Semi-Trapezoidal Method

Fig. 11. Mosquitoes.

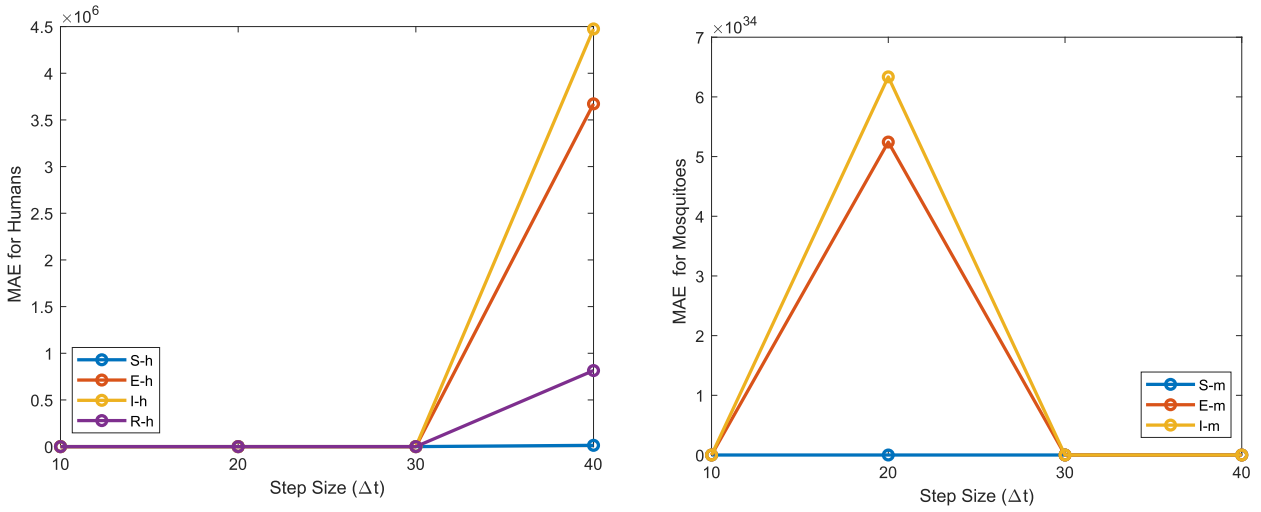

(a) Humans (b) Mosquitoes

Fig. 12. $\Phi(\Delta t) = \Delta t$, MAE for the Explicit Euler Method ($\theta = 0$).

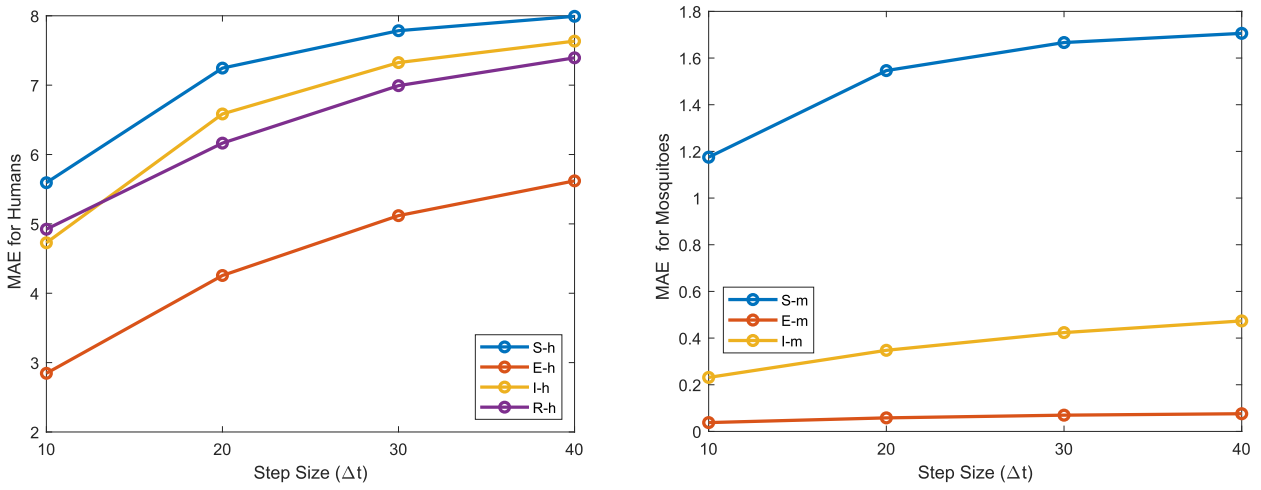

(a) Humans (b) Mosquitoes

Fig. 13. $\Phi_{\frac{1}{h^*(0)}}(\Delta t)$, MAE for the Explicit Euler Method ($\theta = 0$).

humans and mosquitoes, respectively, with the step-size function (60) applied to the semi-trapezoidal method for $\Delta t = 40$. Figure 8(a) depicts the intervals $(0, \frac{\Lambda_h}{\mu_h}]$ and $(0, \frac{\Lambda_m}{\mu_m}]$ are positively invariant for the total populations for humans and mosquitoes, respectively with the step-size function (60) applied to the explicit Euler for adequately large step sizes, $\Delta t = 30$. Figure 8(b) illustrates the intervals $(0, V_h^*)$ and $(0, V_m^*)$ are positively invariant for the total populations, respectively with the step-size function (60) and $\Delta t = 40$ applied to the semi-trapezoidal method. In this example, the total number of humans population remains constant whereas the total number of mosquitoes population declines in the given time. Figures 9 and 10 illustrate property 2 is valid for the step-size function (60). It means that when $C > \frac{1}{h^*(0)}$ in Fig. 9 and $C > \frac{1}{h^{**}(0.5)}$ in Fig. 10, the intervals $(0, \frac{\Lambda_h}{\mu_h}]$ and $(0, \frac{\Lambda_m}{\mu_m}]$ are positively invariant for each component of the solution. The same result is valid for the intervals $(0, V_h^*)$ and $(0, V_m^*)$ for humans and mosquitoes, respectively. Figure 11 shows the results of the step-size function (65) for various C. In Fig. 11(a), the interval $(0, \frac{\Lambda_m}{\mu_m}]$ is positively variant for each component of the solution when $C_0 = 0.06$. The same result is satisfied in Fig. 11(b) for the interval $(0, V_m^*)$ with $C_0 = 0.47$ with $\Delta t = 3$.

In addition to the dynamical consistency, the accuracy of the results is important. In the following, we compare the results obtained by different step-size functions and various step sizes Δt on the time interval [0,1000]. To this end, we generate the reference solution by the ode45 built-in function in MATLAB with the fixed step sizes. Then outcomes are

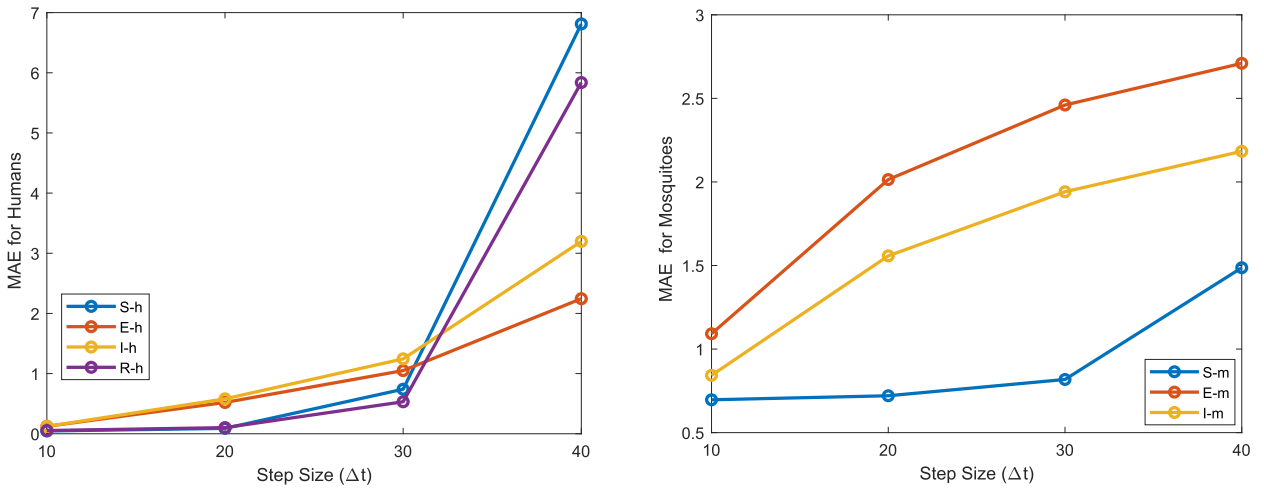

(a) Humans (b) Mosquitoes

Fig. 14. $\Phi(\Delta t) = \Delta t$, MAE for the Semi-Trapezoidal Method ($\theta = 0.5$).

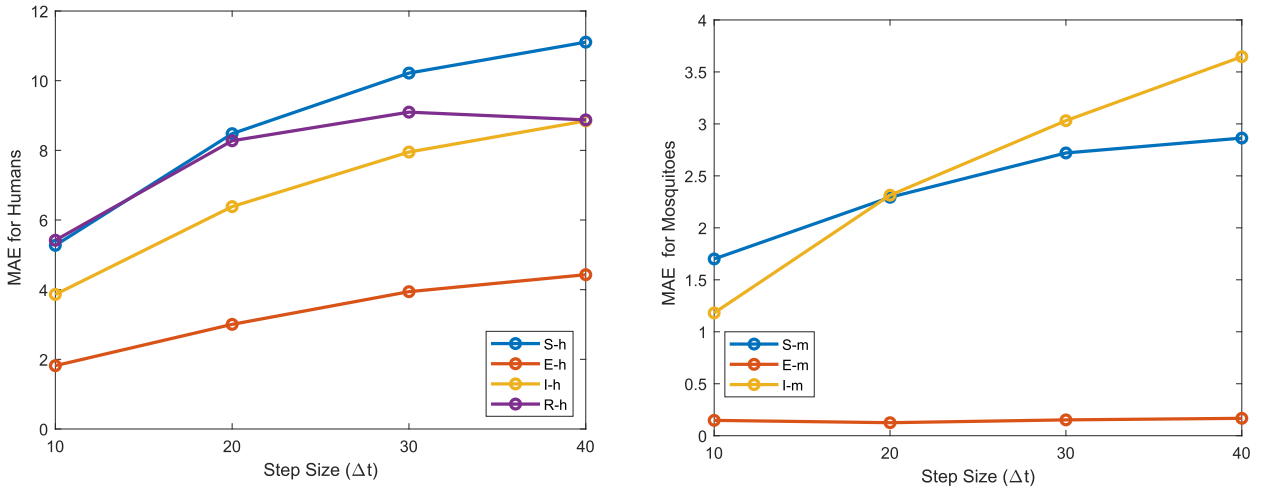

(a) Humans (b) Mosquitoes

Fig. 15. $\Phi_{\frac{1}{h^{**}(0.5)}}(\Delta t)$, MAE for the Semi-Trapezoidal Method ($\theta = 0.5$) .

denoted in maximum absolute error (MAE) graphs to show the efficiency and accuracy of the step-size functions for adequately large step sizes. Figures 12 and 13 compare the maximum absolute errors with various step sizes applied to the explicit Euler method with the step size Δt and step-size function (16) for humans and mosquitoes. The results denote the solution generated by the step-size function (16) is more precise than the result of the step size Δt for sufficiently large step sizes Δt. Figures 14 and 15 visualize the solution of the semi-trapezoidal with the step size Δt method is more accurate than the solution generated by the replacement (16). Figures 16 and 17 illustrate the result obtained by the semi-implicit Euler method with the conventional step size Δt is more accurate than the solution of the step-size function (16) applied to the semi-implicit Euler method. According to Figs. 12–17, it is more accurate to treat the system (17) with the replacement (16) for the explicit Euler method with adequately large step sizes while the step size Δt generates more precise solution for the semi-implicit schemes of the system (17) and we do not need the replacement (16).

The numerical simulations evidence the invariant domains for the step-size functions, $(0, h^*(\theta)]$ and $(0, h^{**}(\theta)]$, are sufficient conditions. For instance, the interval $(0, \frac{\Lambda_m}{\mu_m}]$ is positively invariant for each component of the solution in Fig. 2(a) and the interval $(0, V_m^*)$ is positively invariant in Fig. 4(a) for mosquitoes while $\Phi(\Delta t) \notin (0, h^*(\theta)]$ and $\Phi(\Delta t) \notin (0, h^{**}(\theta)]$, respectively. The step-size function $\Phi_C(\Delta t)$ (16) with $C > 0$ is useful to treat the explicit scheme of the system (17) for sufficiently large step size Δt. In this case, the function $\Phi_C(\Delta t)$ generates more accurate solution than the function $\Phi(\Delta t) =$

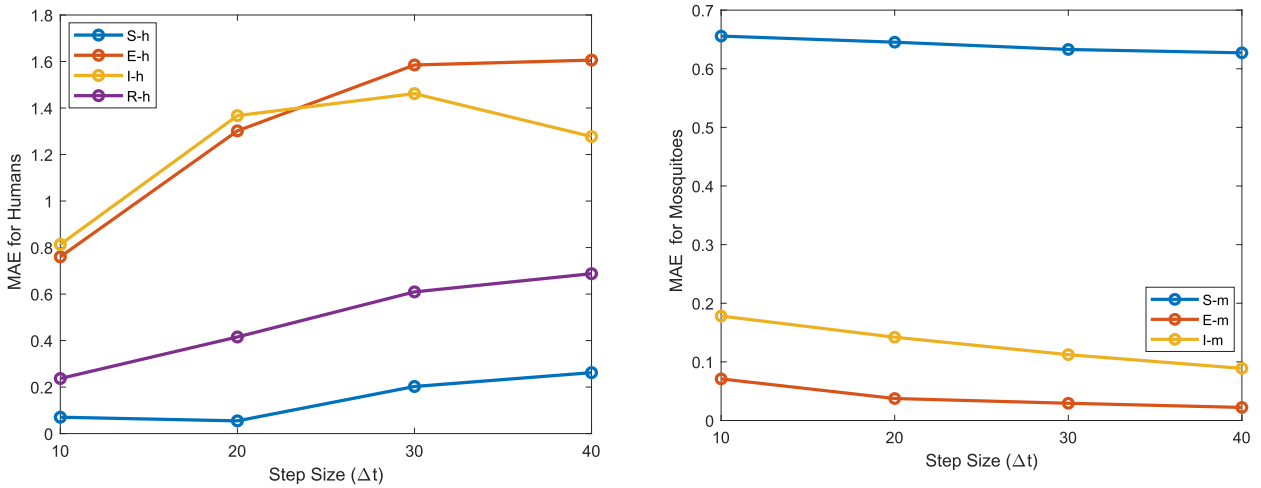

(a) Humans (b) Mosquitoes

Fig. 16. $\Phi(\Delta t) = \Delta t$, MAE for the Implicit Euler Method ($\theta = 1$).

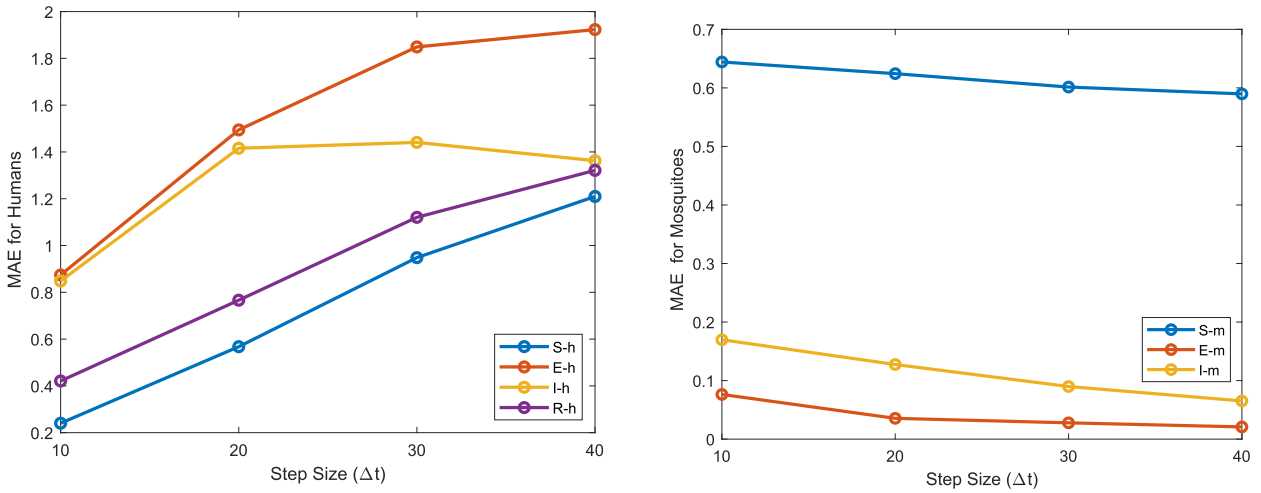

(a) Humans (b) Mosquitoes

Fig. 17. $\Phi_{\frac{1}{R^*(1)}}(\Delta t)$, MAE for the Implicit Euler Method ($\theta = 1$) .

Δt. Figures 12 and 13 visualize the efficiency of the step-size function $\Phi_C(\Delta t)$ for the explicit Euler method with adequately large step sizes Δt. Figures 14–17 illustrate the step-size function $\Phi(\Delta t) = \Delta t$ generates more accurate solution than the function $\Phi_C(\Delta t)$ for the semi-implicit schemes of the system (17).

5. Summary

In this analysis, we consider malaria transmission for infected populations of humans and mosquitoes through the extended Ross model. Since the extended Ross model is a highly nonlinear system, we benefit from numerical methods to approximate its solution. To this end, at the first step, we apply the step-size functions to approximate the time derivatives with the first order consistency. Then we use a nonlocal discretization of the standard θ-method to approximate the right side of the system to obtain a linear system and explicit solution. The results indicate the dynamical consistency highly depends on the step sizes with the step size Δt applied to the Runge–Kutta methods. Since the extended Ross model is a dynamical system, we are interested in analyzing the system on adequately large time intervals. It refers to the small step sizes are not useful. Hence, we suggest a step-size function for the system (17) to preserve the dynamical consistency for any conventional step size Δt. The suggested step-size function improves the accuracy and absolute stability of the explicit

Euler scheme while the nonstandard θ-method generates more precise results with the step-size function $\Phi(\Delta t) = \Delta t$ for the semi-implicit schemes.

Acknowledgments

The research reported in this paper carried out at the Budapest University of Technology and Economics and supported by the NRDI Fund based on the charter of bolster issued by the NRDI Office under the auspices of the Ministry for Innovation and Technology. The paper has been supported by the Hungarian Scientific Research Fund OTKA SNN125119 and also OTKA K137699. The authors are grateful to the unknown referee and also to Prof. Matthias J. Ehrhardt for their fruitful comments and remarks.

References

[1] M.N. Bayoh, S.N. Lindsay, Effect of temperature on the development of the aquatic stages of Anopheles gambiae sensu stricto, Bull. Entomol. Res. 93 (2003) 375–381.
[2] N. Broekhuizen, G.J. Rickard, J. Bruggeman, A. Meister, An improved and generalized second order, unconditionally positive, mass conserving integration scheme for biochemical systems„ Appl. Numer. Math. 58 (3) (2008) 31–340.
[3] F. Chamchod, N.F. Britton, Analysis of a vector-bias model on malaria transmission, Bull. Math. Biol. 73 (2011) 63–657.
[4] N. Chitnisa, J.M. Hyman, J.M. Cushing, Determining important parameters in the spread of malaria through the sensitivity analysis of a mathematical model, Bull. Math. Biol. 70 (2008) 1272–1296.
[5] F. Dorner, R. Mosleh, Analysis of ODE models for malaria propagation, Acta Marisiensis. Seria Technologica 17 (1) (2020) 31–39.
[6] I. Faragó, M. Mincsovics, R. Mosleh, Reliable numerical modelling of malaria propagation, Appl. Math. 63 (2018) 259–271. Springer
[7] I. Faragó, R. Mosleh, Positively invariant semi-implicit discrete model for malaria propagation, in: Annals of the Alexandru Ioan Cuza University of Iaşi (New Series), Mathematics, 2020, pp. 197–214.
[8] M. Ghosha, S. Olaniyi, O.S. Obabiyi, Mathematical analysis of reinfection and relapse in malaria dynamics, Appl. Math. Comput. 373 (2020) 1–18.
[9] K.F. Gurski, A simple construction of nonstandard finite-difference schemes for small nonlinear systems applied to SIR models, Comput. Math. Appl. 66 (2013) 2165–2177.
[10] J. Kima, M. Massoudi, J.F. Antaki, A. Gandinia, Removal of malaria-infected red blood cells using magnetic cell separators: a computational study, Appl. Math. Comput. 218 (12) (2012) 6841–6850.
[11] S. Kopecz, A. Meister, Unconditionally positive and conservative third order modified Patankar-Runge-Kutta discretizations of production-destruction systems, BIT Numer. Math. (2017) 1–38.
[12] A.S. Markus, R.E. Mickens, Suppression of numerically induced chaos with nonstandard finite difference schemes, in: Journal of Computational and Applied Mathematics, vol. 106, Elsevier, 1999, pp. 317–324.
[13] A. Martiradonna, G. Colonna, F. Diele, GeCo: geometric conservative nonstandard schemes for biochemical systems, Appl. Numer. Math. 155 (2020) 38–57.
[14] R.E. Mickens, Nonstandard Finite Difference of Differential Equations, World Scientific Publishing Co. Pte. Ltd, 1994.
[15] R.E. Mickens, Calculations of Denominator Functions for Nonstandard Finite Difference Schemes for Differential Equations Satisfying a Posistivity Condition, Wiely InterScience, 2006, pp. 672–691.
[16] R.E. Mickens, Advances in the Applications of Nonstandard Finite Difference Schemes, World Scientific Publishing Co. Pte. Ltd, 2005.
[17] R. Mosleh, Positivity preservation in explicit discrete malaria model, Ann. Univ. Sci. Budapest. Sect. Math. 63 (2020) 123–133.
[18] S. Nabi, S.S. Qadre, Is global warming likely to cause an increased incidence of malaria? Libyan J. Med. 4 (1) (2009) 18–22.
[19] S. Olaniyi, O.S. Obabiyi, Mathematical model for malaria transmission dynamics in human and mosquito populations with nonlinear forces of infection, Int. J. Pure Appl.Math. 88 (1) (2013) 125–156.
[20] F.U.D. Purwati, J. Nainggolan, Parameter estimation and sensitivity analysis of malaria model, ICoMPAC 2019 1490 (2020) 1–7.
[21] R. Ross, The Prevention of Malaria, John Murray, London, 1911.
[22] L.L.M. Shapiro, S.A. Whitehead, M.B. Thomas, The impact of variations in temperature on early Plasmodium falciparum development in Anopheles stephensi, PLoS Biol. 15 (10) (2017) 1–21.
[23] A.M. Stuart, A.R. Humphries, Dynamical Systems and Numerical Analysis, Cambridge University Pres, 1998.
[24] J. Tumwiine, J.Y.T. Mugisha, L.S. Luboobi, A mathematical model for the dynamics of malaria in a human host and mosquito vector with temporary immunity, Appl. Math. Comput. 189 (2) (2007) 1953–1965.